MODAL ANALYSIS AND DYNAMIC BEHAVIOR FOR ANALYTICAL DRIVETRAIN MODEL

A. Ghorbel M. Abdennadher B. Zghal L. Walha* M. Haddar

Mechanics, Modelling and Manufacturing Laboratory (LA2MP)
Mechanical Engineering Department
National Engineers School of Sfax
Sfax, Tunisia

ABSTRACT

A generalized dynamic model for an automotive drive train system was detailed to investigate its modal properties and dynamic behavior. The model's engine excitation, clutch, gearbox and disc brake were presented. Then, vibration modes were obtained and classified into clutch, transmission system, disc brake, bearing and combined modes. For each vibration mode, the kinetic and strain modal energies distributions were studied. The dynamic equations were resolved using the numerical Newmark method. The dynamic behavior of the bearings and transmission errors for the two gear stages were studied, and, the effect of the disc brake parameters on the transmission error was analyzed. Finally, a frequency sweep analysis was studied to investigate the system resonance problem.

Keywords: Drivetrain vibration, Helical gear, Brake disc, Modal analysis.

1. INTRODUCTION

The vehicle drivability related to its driving comfort plays an important role in a vehicle commercial success. When the drivetrain oscillations are introduced, the drivability of the vehicle is reduced. Since the resulting vibrations are automatically felt by the driver. The need to study their origin has become a must.

The modeling and analysis of the drivetrain system have been the subject of many investigations. Templin P. *et al.* [1] has developed a simple drivetrain model with two inertias. The first presents the engine and transmission, and the second, the wheels and vehicle mass.

In [2], some other linear mathematical models were treated with two masses; representing the engine and the vehicle (including powertrain, clutch and shafts). [3], however, investigated the clutch with certain nonlinear aspects in the modeling of the drivetrain. More detailed and coupled models were also studied in the literature [4-6].

An automobile drive train generally consists of the following main components: engine, gear train, disk brake and transmission shafts. Therefore, understanding and modeling the subsystems allows us to deduce the dynamic behavior of the system. Numerous research works have treated an automotive clutch. Gaillard *et al.* [7] proposed five minimal clutch models and studied the energy dissipation for each of them. Duan *et al.* [8] developed a torsional model for an automotive clutch by converting torque and dry friction disc. Other investigations [9-11] included some nonlinear phenomena to ameliorate the modeling and approach state.

The gear vibration dynamic modeling was investigated by many researchers but the approach of coupling translation and rotation vibrations has been treated only recently. For a more realistic and closer to the experimental values dynamic response, the model has to take into account the flexibility of the shaft and bearings as well as the deformations of the teeth mesh. Besides, the bearing stiffness has a significant effect on the geared system vibration [12, 13] and therefore has to be take into account. Jia S. *et al*. [14] developed a coupled model with 26 degrees of freedom including three shafts and two pairs of gears in mesh to compare damage and localize teeth spalling. An analytical formulation of the gear mesh stiffness taking into consideration the flexibility of the shaft and bearing was developed by [15]. Among the various models presented in literature, the dynamic modeling of a two stage gear reducer has been used lately. Walha L. *et al*. [16] treated a nonlinear dynamic model of a two stage gear system with a mesh stiffness fluctuation. In another work, Walha L. *et al.* [17] developed a model of a helical two stage gear without and with manufacturing defects. This model was then applied to investigate the effects of the eccentricity defect of the mechanical clutch-helical two stage gear [4]. Other researchers used a two stage spur gear reducer to treat the wind turbine gear dynamic behavior in the

* Corresponding author (walhalassaad@yahoo.fr)

DOI : 10.1017/jmech.2017.23
Copyright © 2017 The Society of Theoretical and Applied Mechanics
https://doi.org/10.1017/jmech.2017.23 Published online by Cambridge University Press

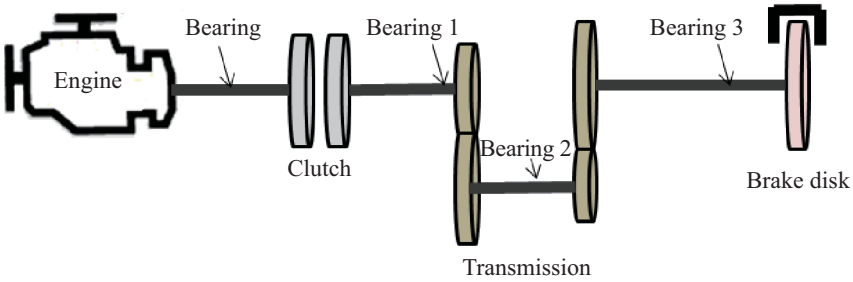


Fig. 1 The general dynamic model of the drivetrain system.

presence of an aerodynamic excitation [18]. On the other hand, Joël Perret-Liaudet [19] proposed some flexible shafts for his one-stage gear model.

Several other investigations were interested in modeling of disc brake to reduce the vibration modes. These can be classified into three categories: The first considered only the pad vibration and neglected the disc effect [20]. The second was only interested in the disc vibration [21-22], whereas the third, known as the coupled model included pad and disc vibrations (*e.g*. Shin's model [23, 24]). Crowther *et al*. [25, 26] proposed a four degree of freedom (DOF) torsional model combining the driveline and brake coupled with a friction pair. Similary, Daogao *et al*. [27] developed a two DOFs model considering the disc torsional and the pad tangential vibrations. Other research works [28] treated a disc brake model taking into account the longitudinal and torsional vibrations of the disc and pads. Li *et al*. [29] proposed a single degree of freedom torsional model with a harmonic excitation, and investigated the actuation force ont he vibration of the system. M. T. Khabou *et al*. [30] studied the influence of the friction phenomenon generated by a disc brake on the dynamic behavior of a single gear stage.

In this paper, the new developed dynamic model with 22 DOF considers the main components of the drivetrain. The natural frequencies and the vibration modes of the drivetrain system are investigated and the modal energy distributions are also discussed for each vibration mode. Finally, the dynamic behavior and the disc brake parameters effecton the transmission error of the geared system were studied. Besides, the system resonance problemwas investigated using the sweep frequency analysis.

2. DRIVETRAIN MODELING

2.1 Model Description

The drivetrain system is an essential element in a vehicle. The main function of the driveline is to convey power from the vehicle's engine to the drive wheels, through a transmission system. The drivetrain system consists of an engine, clutch, gearbox and disc brake. The general dynamic model of the drivetrain system is shown in Fig. 1.

This model is represented by twenty two degrees of freedom. The system is made up of four main blocks. The first presents the engine; the second defines the vehicle clutch; the third describes the two stages of helical geared system and the last one represents the disc brake system. Since the shafts and bearings transmit the mechanical power from the engine to the other components, they will be taken into account in the modeling of the system. Each subsystem model is described in more details in the next section.

2.1.1 Engine Excitation

The system is excited by an engine torque $T_e(t)$. Using Fourier series decomposition, it is written as follows:

$$T_e(t) = T_m + \sum_n T_{pn} \sin(\omega_{pn} + \phi_{pn}) \tag{1}$$

With

$$\omega_{pn} = (N_e / 2)\Omega_e \tag{2}$$

N_e and Ω_e are the number of engine cylinders and the engine velocity. T_{pn} is the amplitude of n^{th} harmonic and ϕ_{pn} is the associated Phase. To simplify the problem, the phase ϕ_{pn} is supposed to be equal to zero. Figure 2 shows the engine torque variation with time.

2.1.2 Clutch Modeling

The second block of the drivetrain system is the clutch. In Fig. 3 a schematic torsional model of a dry clutch in an engaged mode is presented where I_1 represents the torsional flywheel and cover inertia, I_2 is the inertia of the pressure plate, I_3 is the friction disk inertia and I_4 is the clutch hub inertia.

The flywheel and the cover are connected to the pressing plate by a diaphragm spring, which is modeled by a torsional stiffness k_{12}. The connection between the friction disk and the flywheel on one side and pressure plate on the other are respectively modeled by a constant torsional stiffness k_{13} and k_{23}. The torsional stiffness K_1 presents the liaison between the friction disk and clutch hub.

2.1.3 Gearbox Modeling

Figure 4 displays a torsional dynamic model of the third block of the drivetrain system (gearbox). The transmission mechanism is achieved by two helical gear stages. I_{12}, I_{21}, I_{22} and I_{31} are respectively the inertia of gear 12, 21, 22 and 31. The toothed wheels are assumed to be a rigid body and the bearings are modeled

https://doi.org/10.1017/jmech.2017.23 Published online by Cambridge University Press

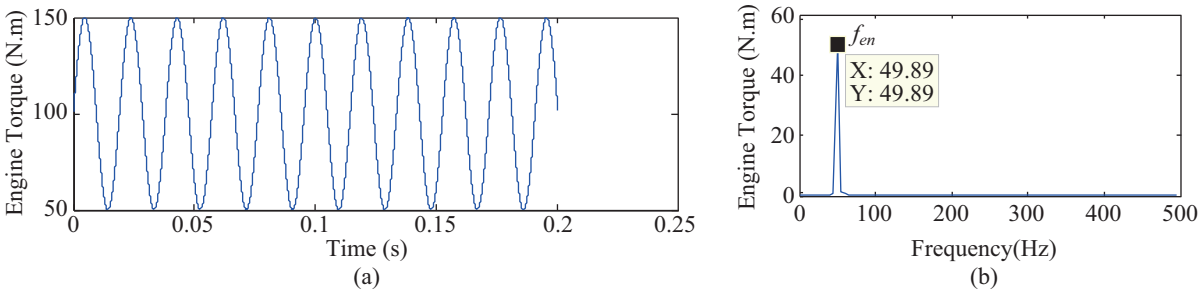


Fig. 2 Engine torque: (a) Time varying engine torque, (b) Frequency spectrum.

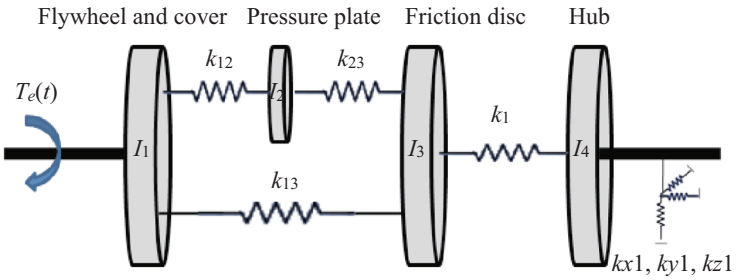


Fig. 3 Dynamic model of the Clutch.

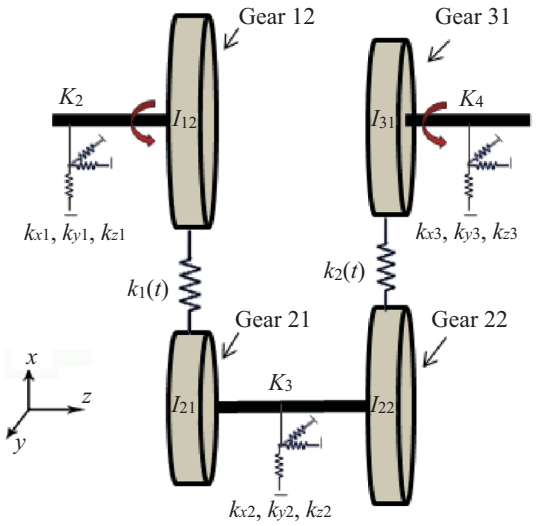


Fig. 4 A two-stage gear dynamic model.

by the linear springs k_{xi}, k_{yi} and k_{zi} of the *i-th* bearing (i = 1, 2, 3). The first stage is linked with the clutch hub by a shaft with the rigidity K_2 and the second stage is associated with the disc brake by another drive shaft with arigidity K_4. The rigidity of the shaft between the two helical gear stages is modeled by the torsional stiffness K_3.

The gear mesh contact for each stage is modeled by a linear time varying stiffness $k_1(t)$ and $k_2(t)$, and a teeth deflection $\delta_1(t)$ and $\delta_2(t)$ following the action line. The periodic variation of the gear mesh stiffness represents another excitation source introduced at the gear and generated by the time varying teeth number in contact. Many research works [4, 17] modeled the time varying stiffness by a periodic trapezoidal form according to time, and represents two mesh frequencies f_{e1} and f_{e2} for two stages of helical gear system. A new approach was developed for the modeling of the gear mesh stiffness in this paper.

The tooth stiffness for both external gears for *i*-stage K_{ei} (i = 1, 2) consists of a Hertzian contact stiffness K_h, a shear stiffness K_s, an axial compressive stiffness K_a and a bending stiffness K_b, which can be expressed as [31]:

$$K_{ei} = \frac{1}{\frac{1}{K_{h,i}} + \frac{1}{K_{s1,i}} + \frac{1}{K_{a1,i}} + \frac{1}{K_{b1,i}} + \frac{1}{K_{s2,i}} + \frac{1}{K_{a2,i}} + \frac{1}{K_{b2,i}}} \tag{3}$$

Where K_h, K_s, K_a and K_b are defined by Z, Wan *et al.* [32]. In this paper, this approach was applied to a helical geared system with the helical angle β.

The gear mesh stiffness of a helical gear includes three approaches corresponding to the contact line change. In the first approach, the helical gear teeth come into contact gradually; the gear mesh stiffness increases with the increase of the contact line length. In the second approach, the contact line length is kept unchanged and the gear mesh stiffness remains relatively stable. In the third approach, the gearmesh stiffness decreases with the contact line length decrease. Figure 5 presents the evolution of the gear mesh stiffness where *a, b* are decimal fractions and *c* is the smallest value among *a* and *b*.

The two gear mesh stiffness as a function of time $k_1(t)$ and $k_2(t)$ and their frequency spectrum are shown in Fig. 6.

The two gear mesh stiffness dephasing depends essen-

https://doi.org/10.1017/jmech.2017.23 Published online by Cambridge University Press

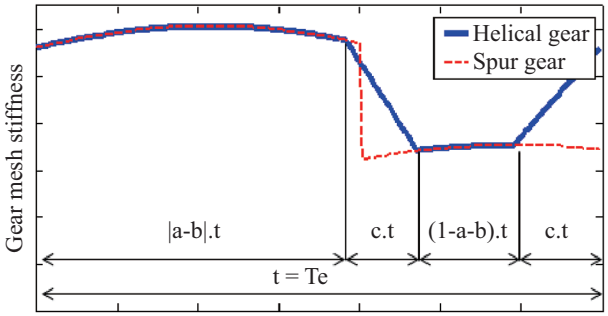


Fig. 5 Evolution of the gearmesh stiffness of helical and spur gear.

tially on the arrangement of the wheels in the reducer and the number of teeth of the toothed wheel 22. The two mesh frequency at teeth contacts f_{e1} and f_{e2} is given by the frequency of the engine speed f_r and the number of teeth Z_{12}, Z_{21} and Z_{22} of the gear 12, 21 and 22, and can be written as follows:

$$f_{e1} = f_r.Z_{12} \tag{4}$$

The two meshing stiffness are connected by the following relationship

$$f_{e2} = \frac{Z_{22}}{Z_{21}} f_{e1} \tag{5}$$

2.1.4 Disc Brake Modeling

Figure 7 displays the suggested linear model of a braking system. Its mechanism involves the phenomenon of dry friction between the components in relative motion. This model is made up of a rigid disc with torsional inertia I_d and two brake pads which are modeled by two masses m_{p1} and m_{p2}, and two torsional inertias I_{p1} and I_{p2}. The frictional contact between the two brake pads and the brake disc is modeled using Coulomb friction theory.

k_{fi} and k_{ti} (i = 1..4) respectively represent the linear axial and torsional stiffness along the Z axis. The pressure applied by the piston to the brake pads is modeled by a static force F_{st}.

2.2 Motion Equation

Lagrange's method was used to formulate the differential equation governing the drivetrain system with 22 degrees of freedom:

$$\{q\} = \{x_1 \quad y_1 \quad z_1 \quad x_2 \quad y_2 \quad z_2 \quad x_3 \quad y_3 \quad z_3 \quad z_{p1} \quad z_{p2} \quad \theta_1 \quad \theta_2 \quad \theta_3 \quad \theta_4 \quad \theta_{12} \quad \theta_{21} \quad \theta_{22} \quad \theta_{31} \quad \theta_d \quad \theta_{p1} \quad \theta_{p2}\} \tag{6}$$

x_i, y_i and z_i are the i-th bearing displacements. z_{p1} and z_{p2} are the pads displacement along the Z- axis. θ is the angular displacement following the Z direction. The motion equation general form is defined by:

$$[M]\{\ddot{q}\} + [C]\{\dot{q}\} + [K_G(t)]\{q\} = \{F(t)\} \tag{7}$$

where M and C are respectively the mass and the damping matrices. $K_G(t)$ is the global stiffness matrix and $\vec{F}(t)$ is the linear vector force.

The mass matrix can be expressed by

$$[M] = \begin{bmatrix} [m] & 0 \\ 0 & [I] \end{bmatrix} \tag{8}$$

where $[m]$ is a matrix made up of the mass terms and $[I]$ is a matrix consisting of the inertia terms.

$$[m] = diag(m_{b1}, m_{b1}, m_{b1}, m_{b2}, m_{b2}, m_{b2}, m_{b3}, m_{b3}, m_{b3}, m_{p1}, m_{p2}) \tag{9}$$

$$[I] = diag(I_1, I_2, I_3, I_4, I_{12}, I_{21}, I_{22}, I_{31}, I_d, I_{p1}, I_{p2}) \tag{10}$$

m_{bi} is the mass of the block i following the direction x, y and $z$and can be expressed as follows:

$$\begin{aligned} m_{b1} &= m_3 + m_4 + m_{12} \\ m_{b2} &= m_{21} + m_{22} \\ m_{b3} &= m_{31} + m_d \end{aligned} \tag{11}$$

For the sake of simplicity, we introduce a damping matrix proportional to the mass and stiffness matrices.

$$[C] = \lambda[M] + \eta[\tilde{K}_G] \tag{12}$$

$\tilde{K}_G$ is the average stiffness independent of time. λ and η are two constants determined by [7, 20].

https://doi.org/10.1017/jmech.2017.23 Published online by Cambridge University Press

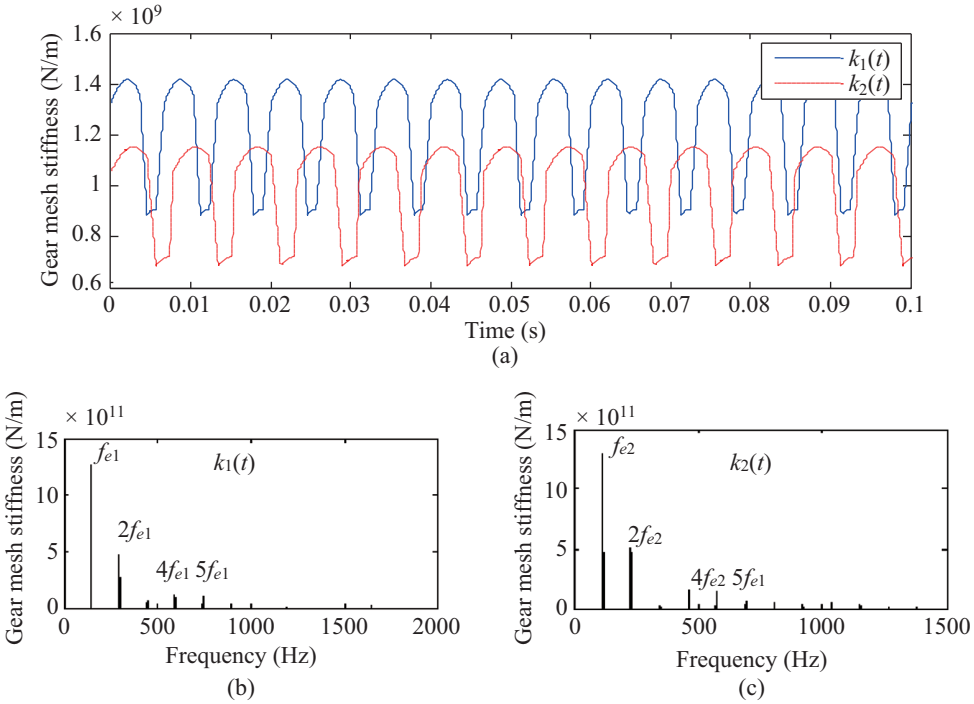


Fig. 6 Gear mesh stiffness model of two helical geared stage: (a) Time varying gear mesh stiffness, (b) Frequency spectrum of $k_1(t)$, (c) Frequency spectrum of $k_2(t)$.

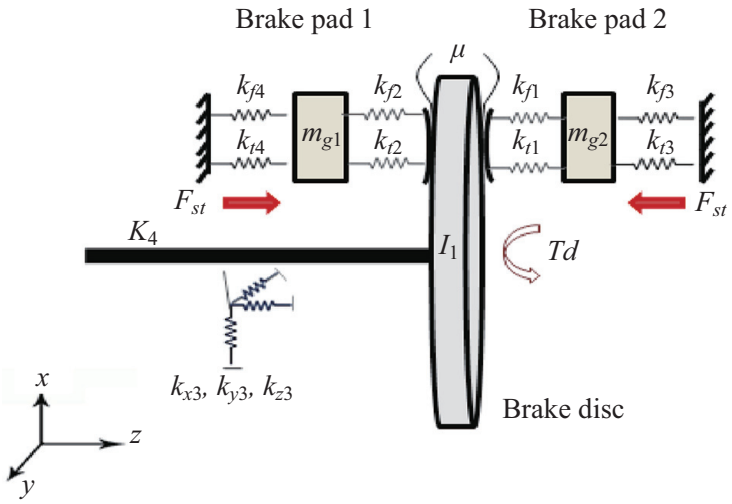


Fig. 7 The disc brake dynamic model.

The stiffness matrix consists of a linear time varying mesh stiffness matrix $K(t)$ and a constant stiffness matrix K_C

$$[K_G(t)] = [K_C] + [K(t)] \tag{13}$$

$$[K_C] = diag([K_{Tran}], [K_{tor}]) \tag{14}$$

where K_{tran} and K_{tor} are respectively the axial and torsional stiffness matrices. These two matrices are defined by equations (15) and (16)

https://doi.org/10.1017/jmech.2017.23 Published online by Cambridge University Press

$$[K_{Tran}]=\begin{bmatrix} k_{x1} & 0 & 0 & 0 & 0 & 0 & 0 & 0 & 0 & 0 & 0 \\ 0 & k_{y1} & 0 & 0 & 0 & 0 & 0 & 0 & 0 & 0 & 0 \\ 0 & 0 & k_{z1} & 0 & 0 & 0 & 0 & 0 & 0 & 0 & 0 \\ 0 & 0 & 0 & k_{x2} & 0 & 0 & 0 & 0 & 0 & 0 & 0 \\ 0 & 0 & 0 & 0 & k_{y2} & 0 & 0 & 0 & 0 & 0 & 0 \\ 0 & 0 & 0 & 0 & 0 & k_{z2} & 0 & 0 & 0 & 0 & 0 \\ 0 & 0 & 0 & 0 & 0 & 0 & k_{x3} & 0 & 0 & 0 & 0 \\ 0 & 0 & 0 & 0 & 0 & 0 & 0 & k_{y3} & 0 & 0 & 0 \\ 0 & 0 & 0 & 0 & 0 & 0 & 0 & 0 & k_{z3}+k_{f1}+k_{f2} & -k_{f1} & -k_{f2} \\ 0 & 0 & 0 & 0 & 0 & 0 & 0 & 0 & -k_{f1} & k_{f1}+k_{f3} & 0 \\ 0 & 0 & 0 & 0 & 0 & 0 & 0 & 0 & -k_{f2} & 0 & k_{f2}+k_{f4} \end{bmatrix} \tag{15}$$

$$[K_{Tor}]=\begin{bmatrix} k_{12}+k_{13} & -k_{12} & -k_{13} & 0 & 0 & 0 & 0 & 0 & 0 & 0 & 0 \\ -k_{12} & k_{12}+k_{23} & -k_{23} & 0 & 0 & 0 & 0 & 0 & 0 & 0 & 0 \\ -k_{13} & -k_{23} & K_1+k_{13}+k_{23} & -K_1 & 0 & 0 & 0 & 0 & 0 & 0 & 0 \\ 0 & 0 & -K_1 & K_1+K_2 & -K_2 & 0 & 0 & 0 & 0 & 0 & 0 \\ 0 & 0 & 0 & -K_2 & K_2 & 0 & 0 & 0 & 0 & 0 & 0 \\ 0 & 0 & 0 & 0 & 0 & K_3 & -K_3 & 0 & 0 & 0 & 0 \\ 0 & 0 & 0 & 0 & 0 & -K_3 & K_3 & 0 & 0 & 0 & 0 \\ 0 & 0 & 0 & 0 & 0 & 0 & 0 & K_4 & -K_4 & 0 & 0 \\ 0 & 0 & 0 & 0 & 0 & 0 & 0 & -K_4 & K_4+k_{t1}+k_{t2} & -k_{t1} & -k_{t2} \\ 0 & 0 & 0 & 0 & 0 & 0 & 0 & 0 & -k_{t1} & k_{t1}+k_{t3} & 0 \\ 0 & 0 & 0 & 0 & 0 & 0 & 0 & 0 & -k_{t2} & 0 & k_{t2}+k_{t4} \end{bmatrix} \tag{16}$$

K_i is the torsional stiffness of the shaft i following the direction θ.

The gear mesh stiffness matrix can be written as follows:

$$[K(t)]=(L_{\delta_1})^T.L_{\delta_1}.k_1(t)+(L_{\delta_2})^T.L_{\delta_2}.k_2(t) \tag{17}$$

where $k_1(t)$ and $k_2(t)$ are the totalmeshing stiffnessat the first and second stages. $L_{\delta 1}$ and $L_{\delta 2}$ are the teeth deflexion and can be written as follows:

$$L_{\delta_1}=\begin{bmatrix} -s_1 & s_2 & s_3 & s_1 & -s_2 & -s_3 & 0 & 0 & 0 & 0 & 0 & 0 & 0 & 0 & 0 & s_4 & s_5 & 0 & 0 & 0 & 0 & 0 \end{bmatrix} \tag{18}$$

$$L_{\delta_2}=\begin{bmatrix} 0 & 0 & 0 & t_1 & -t_2 & t_3 & -t_1 & t_2 & -t_3 & 0 & 0 & 0 & 0 & 0 & 0 & 0 & 0 & t_4 & t_5 & 0 & 0 & 0 \end{bmatrix} \tag{19}$$

The constants of deflection are given by Table 1.

Table 1 $K(t)$ Coefficients

Stage 1	Stage 2
$s_1=\cos\beta.\sin\alpha_1$	$t_1=\cos\beta.\sin\alpha_2$
$s_2=\cos\beta.\cos\alpha_1$	$t_2=\cos\beta.\cos\alpha_2$
$s_3=\sin\beta$	$t_3=\sin\beta$
$s_4=R_{b12}\cos\beta$	$t_4=-R_{b22}\cos\beta$
$s_5=R_{b21}\cos\beta$	$t_5=-R_{b31}\cos\beta$

The vector force is defined by

$$\{F(q,t)\}=\{F_{Tx2/1},F_{Ty2/1},0,0,0,0,0,0,0,F_{st},-F_{st},T_e(t),0,0,0,0,0,0,0,(-T_d-C_{br}),0,0\} \tag{20}$$

The terms $F_{Tx2/1}$ and $F_{Ty2/1}$ are the tangential forces applied by the second block on the first block following the direction x and y, and are given by

https://doi.org/10.1017/jmech.2017.23 Published online by Cambridge University Press

$$F_{Tx2/1} = -\mu_D.P.A; \quad F_{Ty2/1} = -\mu_D.P.A \tag{21}$$

P, A and μ_D are respectively the pressure, the contact area and friction coefficient of the friction torque.

$T_e(t)$ and T_d are respectively the engine torqueand constantload torque.The braking torque can be written as:

$$C_{br} = (F_1 + F_2).r \tag{22}$$

F_1 and F_2 represent the tangential force applied on the brake disc and they can be written as follows

$$F_1 = F_2 = \mu.F_{st} \tag{23}$$

3. MODAL ANALYSIS

The modal analysis can provide the dynamic characteristics of a mechanical system by determining the natural frequencies and vibration modes.

3.1 Natural Frequencies and Vibration Modes

The system is considered invariant of time to investigate the modal properties. The stiffness of two gear-mesh is considered to be equal to their mean values and the damping matrix is neglected. The associated eigen solutions with Eq. (7) can be obtained by solving the following equation

$$\omega_i^2 M\phi_i = \tilde{K}_G.\phi_i \tag{24}$$

Where ω_i are the i-th natural frequencies and ϕ_i is the corresponding vibration mode. M is the mass matrix and $\tilde{K}_G$ is the mean stiffness matrix.

The engine excitation values and the clutch parameters are given in Table 2. The helical geared system and disk brake parameters are listed in Table 3 and Table 4 respectively.

The vibration modes of the drivetrain system can be classified into five types including the clutch mode, transmission mode, disc brake mode, bearing mode and combined mode. The appearance of combined modes is due to the strong coupling between the different blocks. The natural frequencies and their multiplicities associated with each mode type are computed and classified in Table 5. Figure 8 shows the modal deflection of the clutch mode for the natural frequency 201Hz where the

Table 2 Excitation torque and clutch parameters

Parameters and excitation	Values
Torque excitation (N. m)	$T_m = 100$, $T_p = 50$
Engine speed (tr/mn)	500
Friction torque parameters	$P = 8.10^4$ N/m, $A = 0.025$ m^2, $R = 0.07$ m
Masses (kg)	m_1 =5, m_2 =1.17, $m_3 = 0.8$, $m_4 = 0.2$
Inertias (kg m^2)	$I_1 = 0.2$, $I_2 = 12.10^{-3}$, $I_3 = 8.10^{-4}$, $I_4 = 2.10^{-4}$
Torsional stiffness (N m/rad)	$k_{12} = 8.10^4$, $k_{13} = 8.10^4$, $k_{23} = 8.10^4$

Table 3 Geared system parameters

Parameters	Values
Teeth materialcharacteristics	42CrMo4
Density (kg/m^3)	7860
Young module (GPa)	206
Number of teeth	$Z_{12} = 18$; $Z_{21} = 26$; $Z_{22} = 20$; $Z_{31} = 40$
Radius of gears 12, 21, 22, 31 (m)	$R_{b12} = 0.036$; $R_{b21} = 0.052$; $R_{b22} = 0.04$; $R_{b31} = 0.08$
Teeth module (m)	$m = 4.10^{-3}$
Pressure angle	$\alpha_1 = \alpha_2 = 20°$
Helix angle	$\beta = 20°$
Tooth width (m)	$b = 40 \cdot 10^{-3}$
Bearings stiffness (N/m)	$k_x = k_y = k_z = 10^8$

Table 4 Disc brake parameters

Parameters and excitation	Values
Masses (kg)	$m_d = 7.5$, $m_{p1} = 0.2$, $m_3 = 0.2$
Inertias (kg m^2)	$I_d = 0.32$, $I_{p1} = 0.001$, $I_{p2} = 0.001$
Linear stiffness (N/m)	$k_{f1} = k_{f2} = k_{f3} = k_{f4} = 6.10^6$
Torsional stiffness (N m/rad)	$k_{t1} = k_{t2} = k_{t3} = k_{t4} = 3.10^5$

Table 5 Natural frequencies with multiplicity for the system

Vibration mode type	Natural frequencies (Hz)	Multiplicity m
Clutch mode	$f_1 = 19, f_3 = 201$	1
Transmission mode	f_2 =160, $f_6 = 570, f_7 = 585$	1
Disc brake mode	$f_{15} = 1232, f_{16} = 1242,$ $f_{18} = 3898, f_{19} = 3901$	1
Bearing mode	$f_5 = 551, f_{10} = 771$	1
	$f_{13} = f_{14} = 1054$	2
Combined mode	$f_4 = 431, f_8 = 688, f_9 = 751,$ $f_{11} = 782, f_{12} = 988,$ $f_{17} = 1962, f_{20} = 6300,$ $f_{21} = 6953, f_{22} = 9726$	1

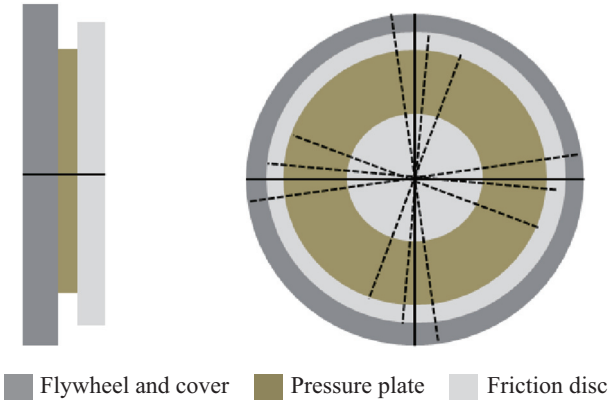


Fig. 8 Vibration modes for clutch in 201 Hz.

https://doi.org/10.1017/jmech.2017.23 Published online by Cambridge University Press

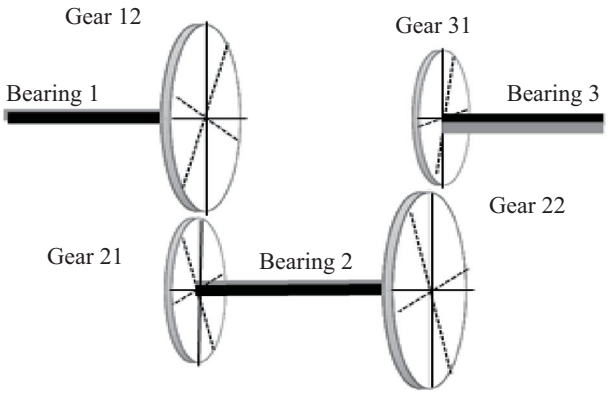


Fig. 9 Vibration modes of the geared system in 570 Hz.

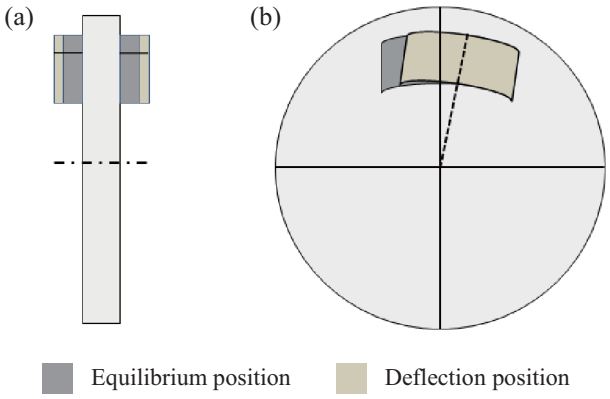


Fig. 10 Vibration modes of disc brake system, (a) translation mode in 1232 Hz, (b) rotation mode in 3898 Hz.

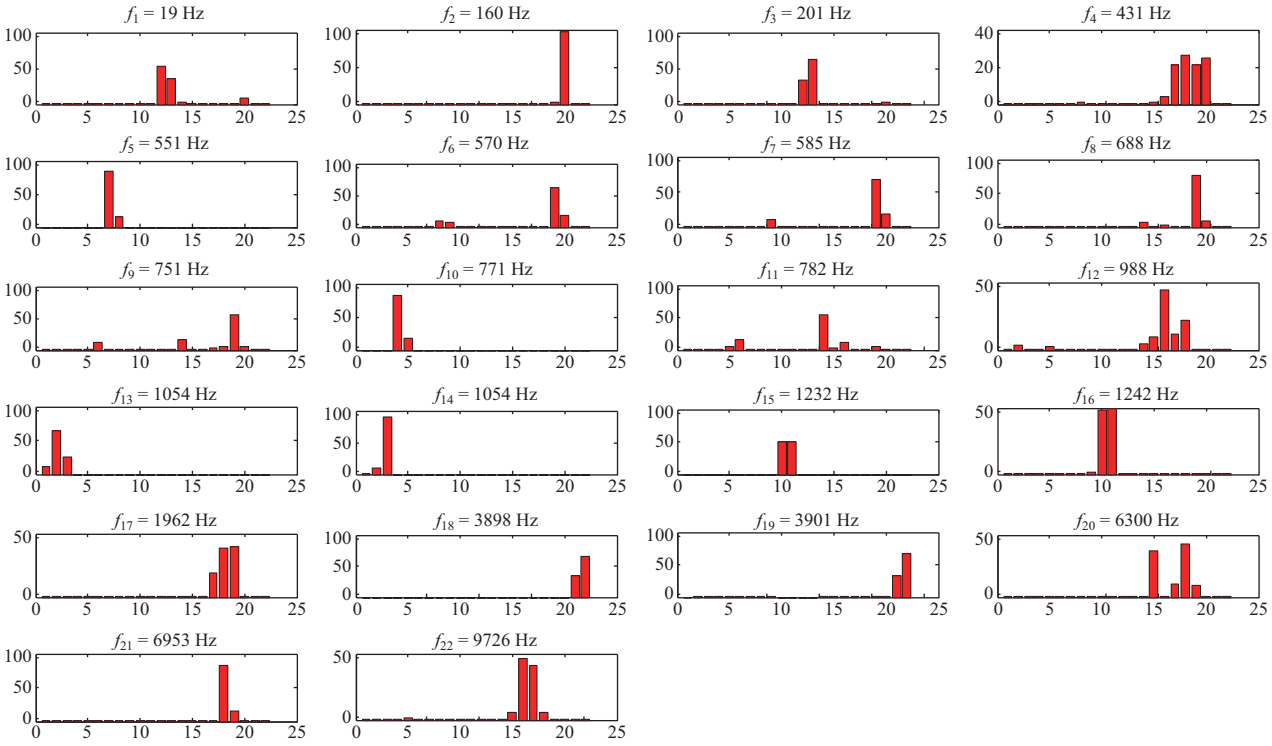


Fig. 11 Kinetic energy distributions.

solid lines represent the equilibrium position and the dotted lines define the deflection position. The front view shows the rotational deflections of the cover and flywheel, pressure plate and friction disc. The side view shows the arrangement of each component. The vibration mode of the clutch hub is negligible compared to the vibration modes of the flywheel and cover, pressure plate and friction disc.

The typical shape of transmission mode at an eigen frequency 570 Hz of the helical geared model is shown in Fig. 9. The solid lines represent the equilibrium position and the dotted lines are the deflection position. From this figure, the transmission mode is remarked to have the following characteristics: (1) Gear 12 has the greatest deflection and gear 31 has the smallest deflection; (2) the rotational deflections of gear 21 and gear 22 are equal; (3) the translation deflections of the three bearings linked of the helical geared system are important especially at the third bearing. From Fig. 10 and Table 5, it can be concluded that the disc brake mode appears in high frequencies.

Figure 10 shows the brake system vibration mode for the natural frequencies 1232 Hz and 3898 Hz. Figure 10(a) presents only the translation mode and the axial deflections of the two pads which have identical values but are in opposite directions. On the contrary, Figure 10(b) presents only the rotation disc brake mode and the rotational deflection of the two pads which also have the same values and opposite directions.

3.2 Modal Kinetic and Modal Strain Energies Distributions

In order to determine the information about deforma-

https://doi.org/10.1017/jmech.2017.23 Published online by Cambridge University Press

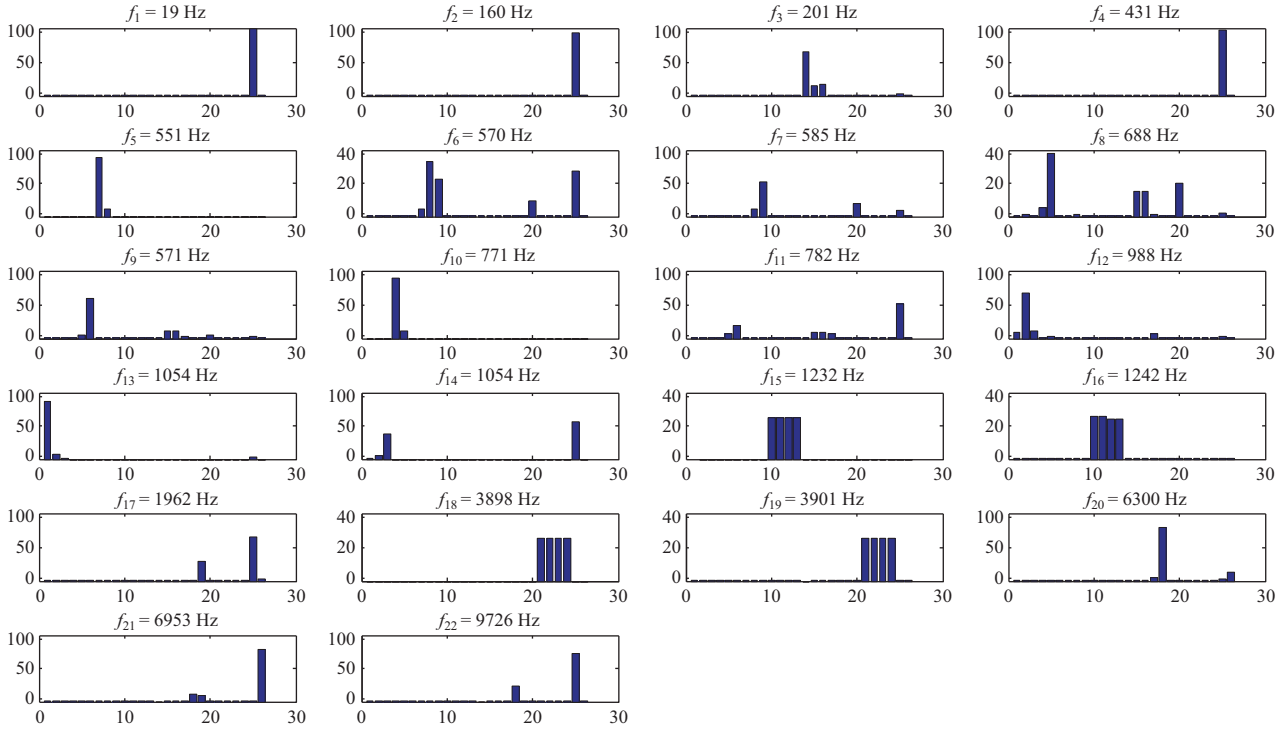


Fig. 12 Strain energy distributions.

Table 6 The *X*-axis location of strain energies

1-3	Bearing 1	14-16	Clutch
4-6	Bearing 2	17-20	Shafts
7-9	Bearing 3	21-24	Rotation of disc brake
10-13	Translation of disc brake	25-26	Meshing geared system

tions and terms of dominant movement of each body at critical speeds (which excite the natural frequencies), one has to calculate the modal kinetic energy and the modal strain energy distributions.

The total modal strain energy can be expressed as follows:

$$Ep_{\phi} = \frac{1}{2}\phi_i^t \tilde{K} \phi_i = \sum Ep_{\phi i} + Ep_{\phi k_1} + Ep_{\phi k_2} \tag{25}$$

where $Ep_{\emptyset i}$ are the strain energiesof the torsional and axial stiffness. $Ep_{\emptyset k1}$ and $Ep_{\emptyset k2}$ are the strain energy of first and second stage meshing.

The modal kinetic energy can also be defined as:

$$Ec_{\phi} = \frac{1}{2}\omega_i^2 \phi_i^t M \phi_i = \sum Ec_{\phi i} \tag{26}$$

where $Ec_{\emptyset i}$ are the strain energy for each DOF in the rotational and translational movements (i = 1..*nDOF*).

Figure 11 shows the distribution percentage of the modal kinetic energies for the 22 natural frequencies. The contribution of each degree of freedom is presented on the *X*-axis. Figure 12 presents the distribution rate of the modal strain energies, where the *X*-axis is defined in Table 6.

The study of the modal deformations and the kinetic and strain energy distributions is very useful in the investigation of the system dynamic behavior. They can explain any increase in the vibration level for certain operating conditions. The modal dominant movement and the dominant strain energy for each frequency are detailed in Table 7.

The drivetrain mode consists of three main blocks; clutch, geared system and disc brake. Figure 13 shows the distribution of the kinetic modal energies and Fig. 14 shows the distribution of strain modal energies in percentages. The *X*-axis defines the contribution of the three blocks. The strain and the kinetic energies are calculated to determine the most excited block for each frequency.

This study allows us to have an idea about the effect of excited sources on the three blocks to control them and reduce their influence on the vibration mode of the entire system.

4. DYNAMIC ANALYSIS OF THE DRIVETRAIN SYSTEM

https://doi.org/10.1017/jmech.2017.23 Published online by Cambridge University Press

Table 7 Dominant motion and dominant strain energy

Frequencies	Modal dominant movement	Dominant strain energy
$f_1 = 19$	Flywheel and cover rotation	Meshing reaction stage 1
$f_2 = 160$	Brake disc rotation	Meshing reaction stage 1
$f_3 = 201$	Pressure plate rotation	Clutch (stiffness k_{12})
$f_4 = 431$	Gear 22 rotation	Meshing reaction stage 1
$f_5 = 551$	Bearing 3 translation along X axis	Bearing 3 along X axis
$f_6 = 570$	Gear 31 rotation	Bearing 3 along Y axis
$f_7 = 585$	Gear 31 rotation	Bearing 3 along Z axis
$f_8 = 688$	Gear 31 rotation	Bearing 2 along Y axis
$f_9 = 751$	Gear 31 rotation	Bearing 2 along Z axis
$f_{10} = 771$	Bearing 2 translation along X axis	Bearing 2 along X axis
$f_{11} = 782$	Friction disc (clutch) rotation	Meshing reaction stage 1
$f_{12} = 988$	Gear 12 rotation	Bearing 1 along Y axis
$f_{13} = 1054$	Bearing 1translation along Y axis	Bearing 1 along X axis
$f_{14} = 1054$	Bearing 1 translation along Z axis	Meshing reaction stage 1
$f_{15} = 1232$	Pad 2 and pad 1 translation	Brake (Translation)
$f_{16} = 1242$	Pad 2 translation	Brake (Translation)
$f_{17} = 1962$	Gear 31 rotation	Meshing reaction stage 1
$f_{18} = 3898$	Pad 2 rotation	Brake (Rotation)
$f_{19} = 3901$	Pad 2 rotation	Brake (Rotation)
$f_{20} = 6300$	Gear 22 rotation	Rotational stiffness bearing 1
$f_{21} = 6953$	Gear 22 rotation	Meshing reaction stage 2
$f_{22} = 9726$	Gear 12 rotation	Meshing reaction stage 1

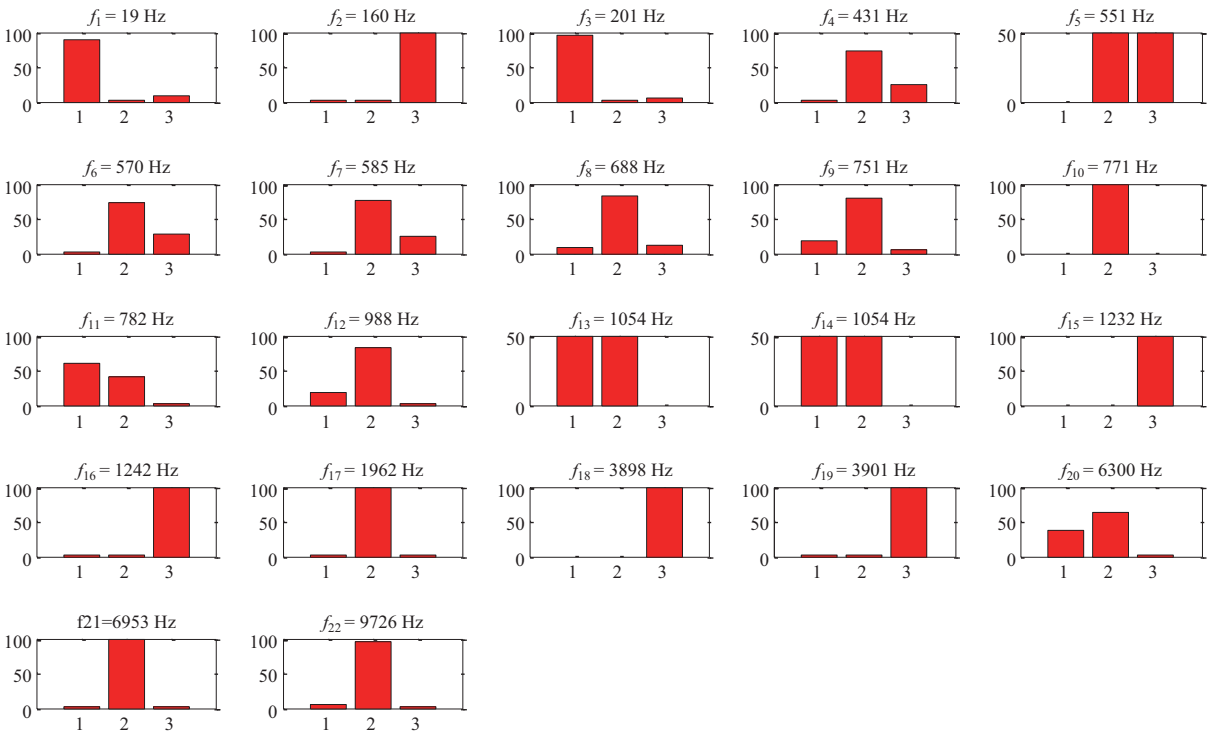


Fig. 13 Kinetic energy distributions for the three block.

https://doi.org/10.1017/jmech.2017.23 Published online by Cambridge University Press

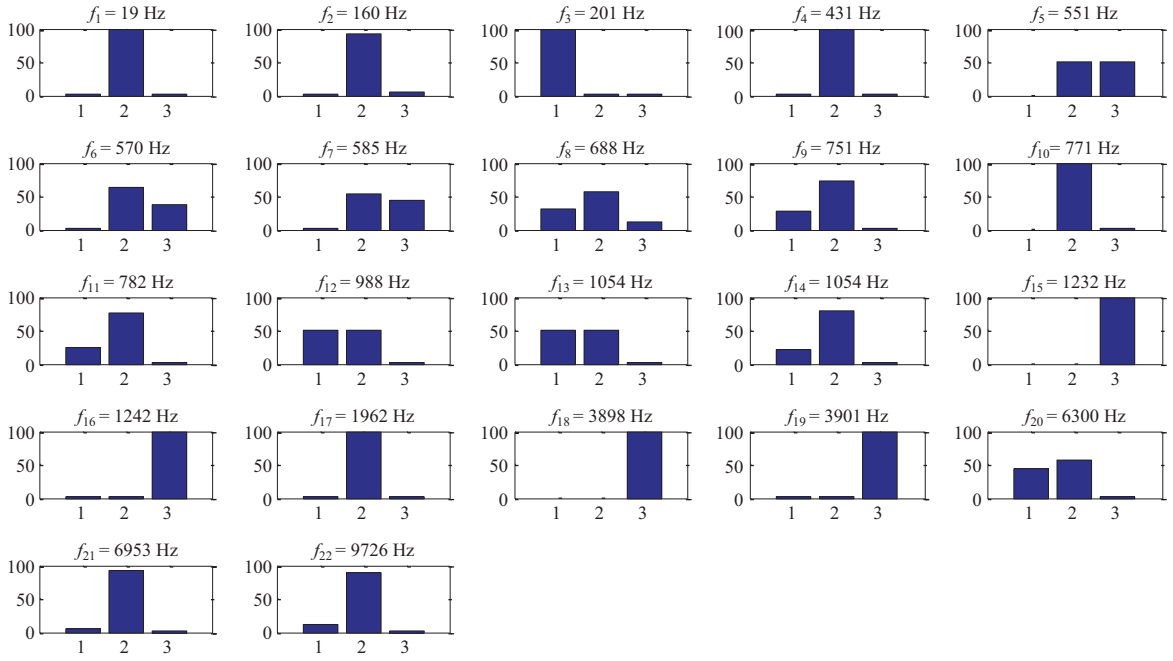


Fig. 14 Strain energy distributions for the three block.

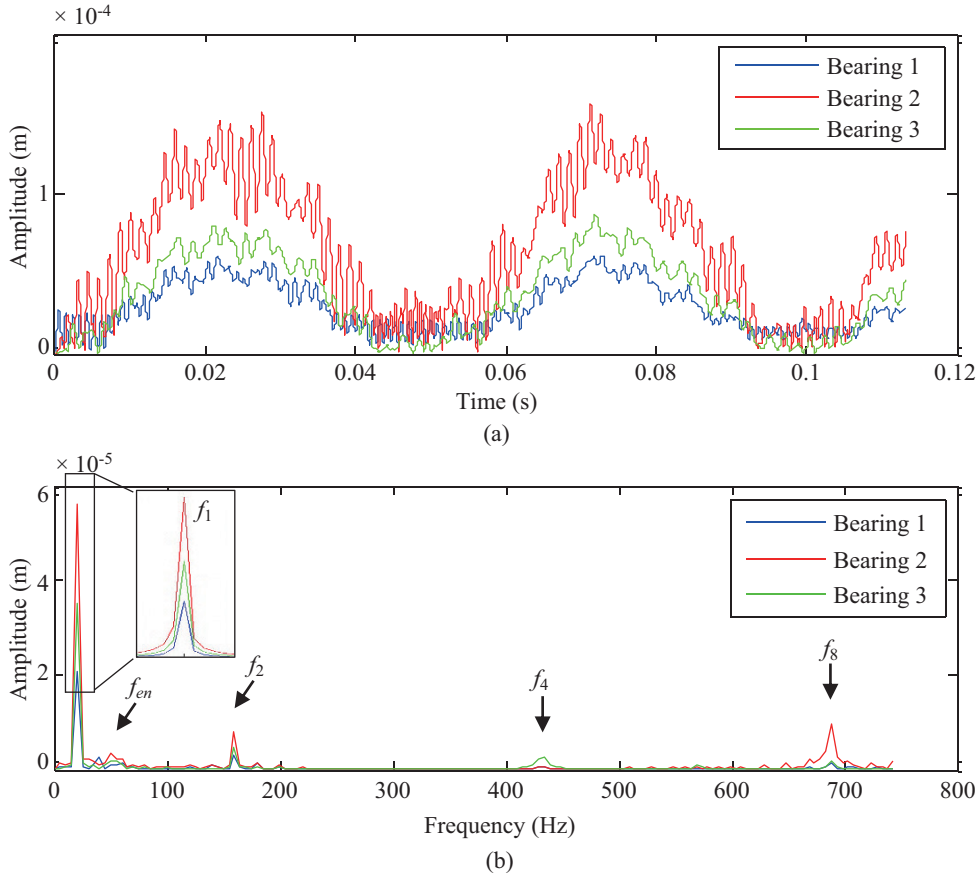


Fig. 15 The resultant displacement of the three bearings: (a) Time response, (b) Frequency spectrum.

In this section, we were first interested in studying the dynamic behavior of the drivetrain system. The Newmark'snumerical method time integration was used to solve the motion equation. The frequency analysis of each discrete time signal can be carried out through the Fourier transform. The Discrete Fourier Transform (DFT) can convert time-domain discrete signal into frequency-domain discrete spectrum. The Fast Fourier Transform (FFT) refers to a very efficient and fast algorithm for computing the DFT [33]. So, the frequency

https://doi.org/10.1017/jmech.2017.23 Published online by Cambridge University Press

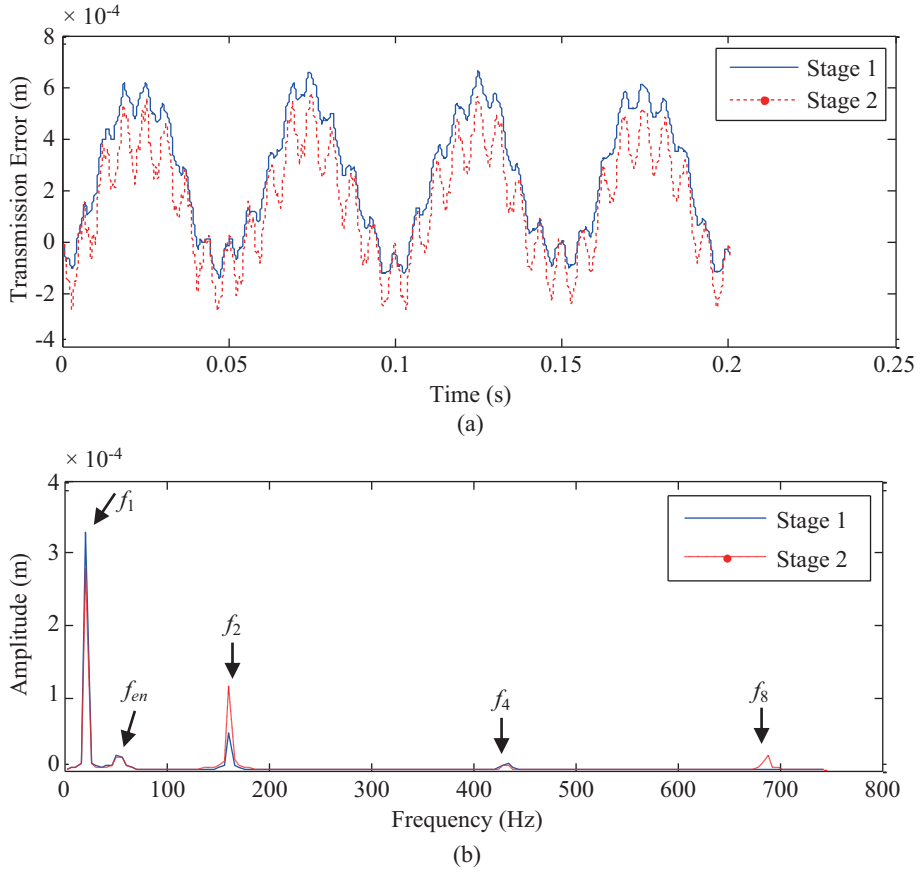


Fig. 16 Transmission error of the two geared stages.

spectrum was obtained using (FFT) algorithm. It shows the time and frequency responses of the bearings and transmission errors. In a second part, the effect of the disc brake parameters on the geared system was investigated. The resonance problem was dealt with using the sweep frequency analysis.

4.1 Dynamic Behavior

The transmission error is the deviation in the position of the driven gear relative to the position it would occupy if both gears were geometrically perfect and undeformed, and can be expressed by the following equation.

$$\delta_1(t) = s_1(x_2 - x_1) + s_2(y_1 - y_2) + s_3(z_1 - z_2) + s_4.\theta_{12} + s_5.\theta_{21} \quad (27)$$

$$\delta_2(t) = t_1(x_2 - x_3) + t_2(y_3 - y_2) + t_3(z_2 - z_3) + t_4.\theta_{22} + t_5.\theta_{31} \quad (28)$$

Where $\delta_1(t)$ and $\delta_2(t)$ are respectively the transmission errors of the first and second stages.

Figure 15 shows the temporal responses of the resultant displacement of three bearings and the corresponding spectrum. The resultant displacement can be expressed by the following equation:

$$R = \sqrt{x_i^2 + y_i^2 + z_i^2} \quad (29)$$

where x_i, y_i and z_i are the i-th bearing displacements along the x, y and z directions.

The most important amplitude returns to the second bearing of the gearbox. If we compared the temporal shape of the bearings 1 and 3, we would note that the fluctuation is more important at bearing 3. This result is due to the difference between the force magnitude applied by the clutch $P.A$ and the static force F_{st} applied by the disc brake on the bearings.

The natural frequencies and the engine excitation frequency f_{en} are clear enough on the spectrum signal. These frequencies are the most dominant in dynamic responses of the system.

Figure 16 shows the transmission error of the two geared stages and the corresponding spectrum. We conclude that the amplitude of the first stage is slightly greater than the second one.

4.2 Parametric Study

In this part, the effect of adding a brake mechanism to the geared system and especially on the transmission error was investigated. A parametric study was achieved to different torsional stiffness values k_t related to the brake pad shown in Fig. 17 and Fig. 18.

These two figures present the significant effect of the torsional stiffness on the transmission error of the two stages. This effect is found to be more important with small stiffness values. However, the linear stiffness k_f has a negligible impact.

The friction coefficient between disc and pad has less

https://doi.org/10.1017/jmech.2017.23 Published online by Cambridge University Press

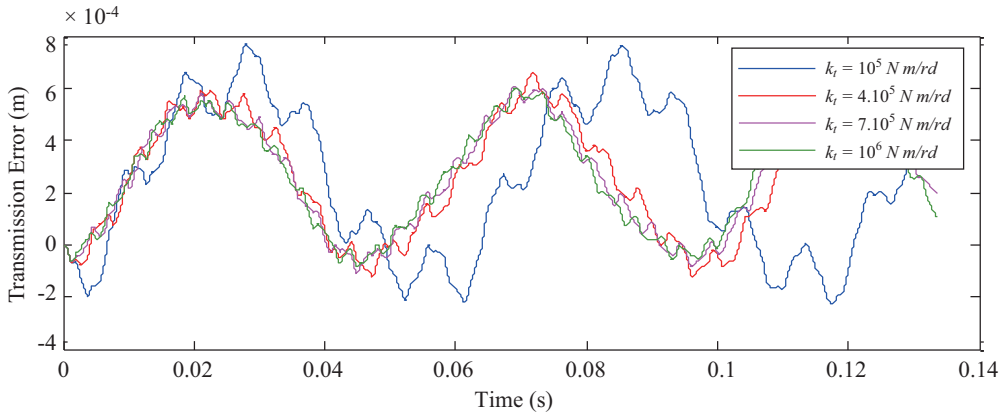


Fig. 17 First stage transmission error for a varying k_t.

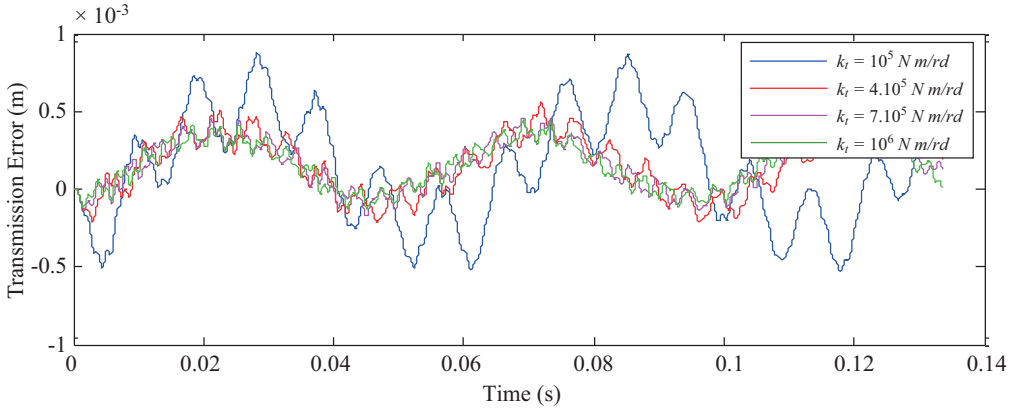


Fig. 18 Second stage transmission error for a varying k_t.

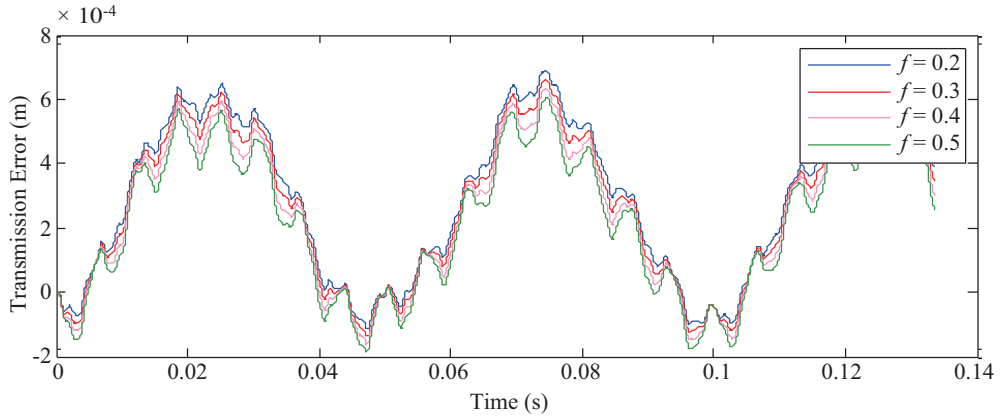


Fig. 19 Transmission error for varying friction coefficient μ of the first stage.

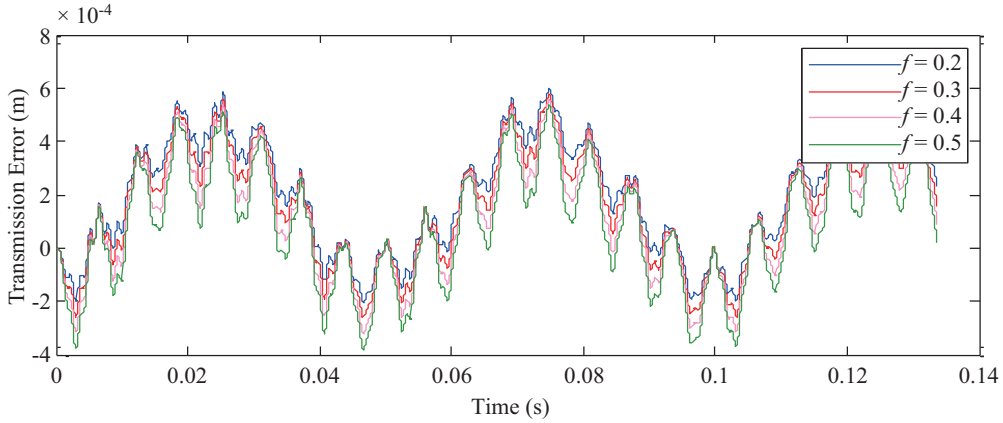


Fig. 20 Transmission error for varying friction coefficient μ of the second stage.

https://doi.org/10.1017/jmech.2017.23 Published online by Cambridge University Press

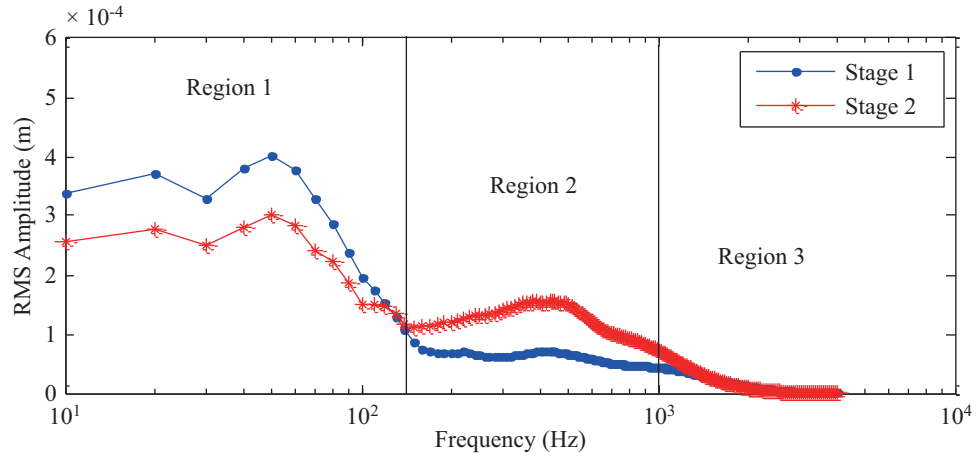


Fig. 21 Sweep frequency response of two geared stage.

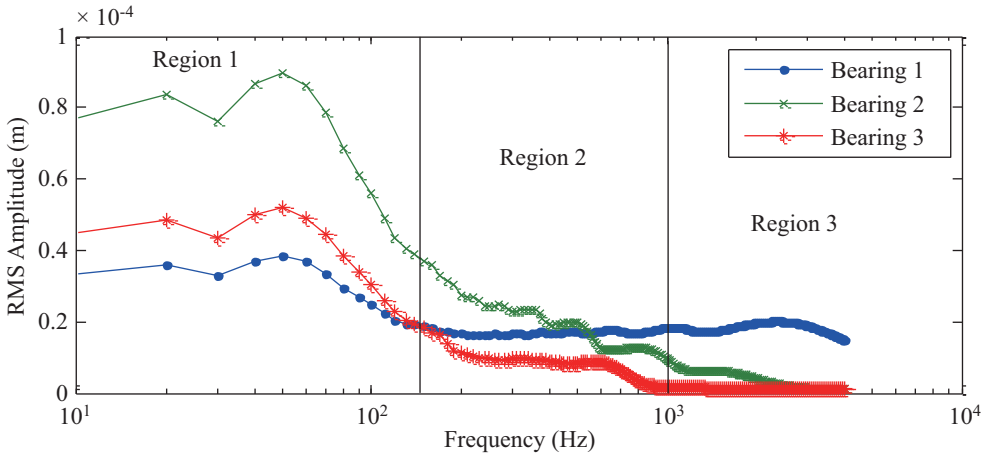


Fig. 22 Sweep frequency response of three bearings.

effect when compared to the torsional stiffness of the disc brake (Figs. 19 and 20). We can conclude that the signal periodicity is more remarkable with a higher friction coefficient.

4.3 Frequency Sweep Analysis

To investigate the system resonance problem, a frequency sweep analysis of the engine torque T_e was studied. In this section, a frequency study of the three bearings and the transmission error of the two stages were presented. The Root Mean Square (RMS) values of the time domain vibration signals were used to measure the amplitudes for each frequency. Figure 21 presents the sweep frequency response of a two geared stage.It shows that the largest vibrations correspond to lower frequencies. The first geared stage vibration is more important at low frequencies (region 1). In the medium band frequency (region 2), the second geared stage vibration is the higher than the first stage one. For the high frequency (region 3), the vibrations of the two stages are similar and are the lowest with respect to the two preceding frequency bands.

The sweep frequency responses of the three bearings are shown in Fig. 22 indicating three distinct band frequency regions:

- Region 1: the vibration level of the three bearings is the highest. Bearing 2 located between the two geared stages has the greatest RMS amplitude.
- Region 2: when frequency is increased, the amplitude of the first bearing becomes more important than that of the first.
- Region 3: the vibration of the first bearing becomes higher.

5. CONCLUSIONS

In this work, a new drive train model involving an engine excitation, clutch, helical geared system and disc brake was developed. Lagrange formalism was used to formulate the differential equation. The study of the drivetrain system was achieved using two approaches; the modal analysis and the dynamic analysis. Con-

https://doi.org/10.1017/jmech.2017.23 Published online by Cambridge University Press

cerning the modal analysis approach, the natural frequencies and vibration modes were obtained revealing that they can be classified into five main modes: clutch mode, transmission mode, disc brake mode, bearing mode and combined mode. When studying the kinetic and strain modal energies distributions, another classification appeared depending on the dominant energy for each natural frequency and can be divided into three main blocks: clutch, geared system and disc brake. In the other analysis approach, the dynamic behavior of the bearings and the transmission error of the two geared stages were presented. In addition, the effects of the disc parameters (torsional and linear stiffness and friction coefficient) in the two transmission errors were investigated. The torsional stiffness was noticed to have the most significant effect. Finally, the resonance problem was investigated using the frequency sweep analysis.

NOMENCLATURE

$T_e(t)$	Engine torque excitation;
T_m	Average engine torque;
T_{pn}	Amplitude of n-th harmonic;
N_e	Number of cylinders of the engine;
ω_{pm}	Pulsation of n-th harmonic;
Ω_e	Engine speed;
ϕ_{pm}	Phase of n-th harmonic;
I_1	Inertia of flywheel and cover;
I_2	Inertia of the pressure plate;
I_3	Inertia of the friction disk;
I_4	Inertia of the hub of the clutch;
I_{12}, I_{21}, I_{22}, I_{31}	Inertia of gear 12, 21, 22 and 31;
I_d	Inertia of brake disc;
I_{p1}, I_{p2}	Inertia of the two brake pads;
m_1	Mass of flywheel and cover;
m_2	Mass of the pressure plate;
m_3	Mass of the friction disk;
m_4	Mass of the hub of the clutch;
m_{21}, m_{22}	Masses of gear 21, 22;
m_{31}	Mass of gear 31;
m_d	Mass of disc brake;
m_{b1}, m_{b2}, m_{b3}	Masses of blocks 1, 2, 3;
k_{x1}, k_{y1}, k_{z1}	Linear stiffness of the bearing 1;
k_{x2}, k_{y2}, k_{z2}	Linear stiffness of the bearing 2;
k_{x3}, k_{y3}, k_{z3}	Linear stiffness of the bearing 3;
k_{fi} (i = 1..4)	Linear stiffness of disc brake;
k_{12}	Torsional stiffness between the cover and pressing plate;
k_{13}	Torsional stiffness between the friction disc and the flywheel;
k_{23}	Torsional stiffness between the friction disc and the pressure plate;
K_1	Torsional stiffness between friction disc and clutch hub;
K_2, K_3, K_4	Torsional stiffness of the bearings 1, 2, 3;
k_{ti} (i = 1..4)	Torsional stiffness of disc brake;
$k_1(t)$, $k_2(t)$	Gear mesh stiffness of geared stage 1 and 2;
δ_1(t), $\delta_2(t)$	Transmission error of the two geared stage;
K_{ei} (i = 1, 2)	The tooth stiffness for both external gears for i-stage;
K_h	Hertziancontact stiffness;
K_s	Shear stiffness;
K_a	Axial compressive stiffness;
K_b	Bending stiffness;
a, b	Decimal fractions;
c	The smallest of a and b;
f_{e1}, f_{e2}	Gear mesh frequencies of the two stage of helical gear;
f_r	Frequency of rotation of the engine;
f_e	Frequency of the engine torque;
f_i (i = 1..22)	The natural frequencies;
Z_{12}, Z_{21}, Z_{22}, Z_{31}	Number of teeth of gear 12, 21, 22 and 31;
$[M]$	Global mass matrix;
$[C]$	Global damping matrix;
$[K_G(t)]$	Global stiffness matrix;
$[K_{Tran}]$	Axial stiffness matrix;
$[K_{Tor}]$	Torsional stiffness matrix;
$[m]$	Mass matrix;
$[I]$	Inertia matrix;
$\{F_e(t)\}$	Linear vector force;
$\{q\}$, $\{\dot{q}\}$, $\{\ddot{q}\}$	Displacement vector, speed vector and acceleration vector;
x_i, y_i, z_i	The i-th bearing displacements;
z_{p1}, z_{p2}	Pads displacement along Z- axis;
θ_i	Angular displacement following Z direction;
$\tilde{K}_G$	Average stiffness;
λ, η	Two constants determined experimentally;
K_c	Constant stiffness matrix;
K_{tran}	Axial stiffness matrix;
K_{tor}	Torsional stiffness matrix;
$L_{\delta 1}$, $L_{\delta 2}$	Vectors of the teeth deflection;
s_i (i =1..5)	Constants of the teeth deflection of stage 1;
t_i (i = 1..5)	Constants of the teeth deflection of stage 2;
α_i	Pressure angle of the gear of stage i;
β	Helix angle of the gear;
R_{b12}, R_{b21}, R_{b22}, R_{b31}	Radius of gear 12, 21, 22, 31;
$F_{Tx2/1}$, $F_{Ty2/1}$	The tangential forces following the direc-

https://doi.org/10.1017/jmech.2017.23 Published online by Cambridge University Press

	tion x and y;
μ_D, μ	Friction coefficient of the clutch and the disc brake;
P, A	Pressure and area contact of the friction torque;
F_{st}	Static force applied by the piston on the brake pads;
T_d	Constant load torque;
C_{br}	Braking torque;
F_1, F_2	Tangential forces applied on the brake disc;
r	Radius contact point between the pads and the center of the disc;
ω_i	Pulsation of i-th natural frequency;
ϕ_i	Mode vibration of i-th natural frequency;
$Ep_{ø}$	Total modal strain energy;
$Ec_{ø}$	Total modal kinetic energy;
$Ep_{øi}$	Strain energies of the torsional and axial stiffness;
$Ep_{øk1}$, $Ep_{øk2}$	Strain energy of first and second stage meshing gear;
$Ec_{øi}$	Strain energy of each DOF in the rotational and translational movement;
DOF	Degree of freedom;
RMS	Root mean square;
FFT	Fast Fourier Transform;
DFT	Discrete Fourier Transform

REFERENCES

1. Templin, P. and Egardt, B., "An LQR Torque Compensator for Driveline Oscillation Damping," *18th IEEE International Conference Control Applications*, pp. 352-356 (2009).
2. Bemporad, A., Borrelli, F., Glielmo, L. and Vasca, F., "Optimal Piecewise-Linear Control of Dry Clutch Engagement," *IFAC Workshop Advances in Automotive Control*, pp. 33-38 (2001).
3. Heijden, A. V. D., Serrarens, A. F. A., Camlibel, M. K. and Nijmeijer, H., "Hybrid Optimal Control of Dry Clutch Engagement," *International Journal of Control*, **80**, pp. 1717-1728 (2007).
4. Walha, L., Driss, Y., Khabou, M. T., Fakhfakh, T., and Haddar, M., "Effects of Eccentricity Defect on the Nonlinear Dynamic Behavior of the Mechanism Clutch-Helical Two Stage Gear," *Mechanism and Machine Theory*, **46**, pp. 986-997 (2011).
5. VanBerkel, K., Hofman, T., Serrarens, A. and Steinbuch, M., "Fast and Smooth Clutch Engagement Control for Dual-Clutch Transmissions," *Control Engineering Practice*, **22**, pp. 57-68 (2014).
6. Caruntu, C. F., Lazar, M. and Di Cairano, S., "Driveline Oscillations Damping: A Tractable Predictive Control Solution Based on a Piecewise Affine Model," *Nonlinear Analysis: Hybrid Systems*, **19**, pp. 168-185 (2016).
7. Gaillard, C. L. and Singh, R., "Dynamic Analysis of Automotive Clutch Dampers," *Applied Acoustics*, **60**, pp. 399-424 (2000).
8. Duan, C. and Singh, R., "Dynamics of a 3 DOF Torsional System with a Dry Friction Controlled Path," *Journal of Sound and Vibration*, **289**, pp. 657-688 (2006).
9. Kim, T. C., Rook, T. E. and Singh, R., "Super- and Sub-Harmonic Response Calculations for a Torsional System with Clearance Nonlinearity Using the Harmonic Balance Method," *Journal of Sound and Vibration*, **281**, pp. 965-993 (2005).
10. Kim, T. C., Rook, T. E. and Singh, R., "Effect of Nonlinear Impact Damping on the Frequency Response of a Torsional System with Clearance," *Journal of Sound and Vibration*, **281**, pp. 995-1021 (2005).
11. Driss, Y., Fakhfakh, T. and Haddar, M., "Effect of Eccentricity on a Clutch System under a Harmonically Varying Normal Load," *Journal of Failure Analysis and Prevention*, **7**, pp. 127-136 (2007).
12. Kim, W., Yoo, H. H. and Chung, J., "Dynamic Analysis for a Pair of Spur Gears with Translational Motion Due to Bearing Deformation," *Journal of Sound and Vibration*, **329**, pp. 4409-4421 (2010).
13. Howard, I., Jia, S. and Wang, J., "The Dynamic Modelling of a Spur Gear in Mesh Including Friction and a Crack," *Mechanical Systems and Signal Processing*, **15**, pp. 831-853 (2001).
14. Jia, S. and Howard, I., "Comparison of Localized Spalling and Crack Damage from Dynamic Modelling of Spur Gear Vibrations," *Mechanical Systems and Signal Processing*, **20**, pp. 332-349 (2006).
15. Chaari, F., Baccar, W., Abbes, M. S. and Haddar, M., "Effect of Spalling or Tooth Breakage on Gearmesh Stiffness and Dynamic Response of a One-Stage Spur Gear Transmission," *European Journal of Mechanics-A/Solids*, **27**, pp. 691-705 (2008).
16. Walha, L., Fakhfakh, T. and Haddar, M., "Nonlinear Dynamics of a Two-Stage Gear System with Mesh Stiffness Fluctuation, Bearing Flexibility and Backlash," *Mechanism and Machine Theory*, **44**, pp. 1058-1069 (2009).
17. Walha, L., Driss, Y., Fakhfakh, T. and Haddar, M., "Effect of Manufacturing Defects on the Dynamic Behaviour for an Helical Two-Stage Gear System," *Mécanique & Industries*, **10**, pp. 365-376 (2009).
18. Abboudi, K. *et al*., "Dynamic Behavior of a Two-Stage Gear Train Used in a Fixed-Speed Wind Turbine," *Mechanism and Machine Theory*, **46**, pp. 1888-1900 (2011).
19. Perret-Liaudet, J., "An Original Method for Computing the Response of a Parametrically Excited

https://doi.org/10.1017/jmech.2017.23 Published online by Cambridge University Press

Forced System", *Journal of Sound and Vibration*, **196**, pp. 165-177 (1996).

20. Oberst, S. and Lai, J. C. S., "Statistical Analysis of Brake Squeal Noise," *Journal of Sound and Vibration*, **330**, pp. 2978-2994 (2011).
21. Ouyang, H., Mottershead, J. E., Cartmell, M. P. and Brookfield, D. J., "Friction-Induced Vibration of an Elastic Slider on a Vibrating Disc," *International Journal of Mechanical Sciences*, **41**, pp. 325-336 (1999).
22. Von Wagner, U., Hochlenert, D. and Hagedorn, P., "Minimal Models for Disk Brake Squeal," *Journal of Sound and Vibration*, **302**, pp. 527-539 (2007).
23. Shin, K., Brennan, M. J., Oh, J. E. and Harris, C. J., "Analysis of Disc Brake Noise Using a Two-Degree-of-Freedom Model," *Journal of Sound and Vibration*, **254**, pp. 837-848 (2002).
24. Shin, K., Oh, J. E. and Brennan, M. J., "Nonlinear Analysis of Friction Induced Vibrations of a Two-Degree-of-Freedom Model for Disc Brake Squeal Noise," *JSME International Journal Series C Mechanical Systems, Machine Elements and Manufacturing*, **45**, pp. 426-432 (2002).
25. Crowther, A. R. and Singh, R., "Analytical Investigation of Stick-Slip Motions in Coupled Brake-Driveline Systems," *Nonlinear Dynamics*, **50**, pp. 463-481 (2007).
26. Crowther, A. R. and Singh, R., "Identification and Quantification of Stick-Slip Induced Brake Groan Events Using Experimental and Analytical Investigations," *Noise Control Engineering Journal*, **56**, pp. 235-255 (2008).
27. Wei, D., Ruan, J., Zhu, W. and Kang, Z., "Properties of Stability, Bifurcation, and Chaos of the Tangential Motion Disk Brake," *Journal of Sound and Vibration*, **375**, pp. 353-365 (2016).
28. Ahmed, I., "Analysis of Disc Brake Squeal Using a Ten-Degree-of-Freedom Model," *International Journal of Engineering, Science and Technology*, **3**, pp. 142-155 (2011).
29. Chen, L. and Xi, G., "Stability and Response of a Self-Amplified Braking System under Velocity-Dependent Actuation Force," *Nonlinear Dynamics*, **78**, pp. 2459-2477 (2014).
30. Khabou, M. T. *et al*., "Influence of Disk Brake Friction on the Dynamic Behaviour of a Directly Coupled Spur Gear Transmission," *Multidiscipline Modeling in Materials and Structures*, **10**, pp. 146-162 (2014).
31. Tian, X. H., "Dynamic Simulation for System Response of Gearbox Including Localized Gear Faults," *Master's Thesis, University of Alberta* (2004).
32. Wan, Z., Cao, H., Zi, Y., He, W. and Chen, Y., "Mesh Stiffness Calculation Using an Accumulated Integral Potential Energy Method and Dynamic Analysis of Helical Gears," *Mechanism and Machine Theory*, **92**, pp. 447-463 (2015).
33. Cooley, J. W. and Tukey, J. W., "An Algorithm for the Machine Calculation of Complex Fourier Series," *Mathematics of Computation*, **19**, pp. 297-301 (1965).

(Manuscript received September 5,2016,
accepted for publication February 21, 2017.)

https://doi.org/10.1017/jmech.2017.23 Published online by Cambridge University Press